Performance characteristics of a new structured packing

Vincent Bessou [a], David Rouzineau [a,*], Michel Prévost [a], François Abbé [b], Charles Dumont [b], Jean-Pierre Maumus [b], Michel Meyer [a]

[a] Université de Toulouse, INPT, ENSIACET, Laboratoire de Génie Chimique, UMR 5503, 5 rue Paulin Talabot, 31106 Toulouse Cedex 01, France
[b] SNECMA/SPS Les Cinq Chemins, 33187 LeHaillan Cedex, France

A B S T R A C T

A new structured packing using carbon fibres, called Sepcarb® 4D, is presented. This packing has several attractive properties, such as high voidage (ε=94%) and high effective area (a=420 $m^2\,m^{-3}$). These properties are advantageous for packing used as a gas–liquid contactor for separation units. To determine the internal characteristics of this packing, we performed several experiments using a 150-mm-internal-diameter column. Firstly, hydrodynamics experiments were conducted using an air–water counter current flow to determine the pressure drop (for both dry and wet packing) and flooding point. Secondly, the mass transfer efficiency was determined in terms of HETP (height equivalent to theoretical plate) by total reflux experiments with an n-heptane/cyclohexane mixture at atmospheric pressure. Hydrodynamic performance and mass transfer efficiency were compared with those of packings generally used in distillation and absorption.

1. Introduction

For separation operations using packed columns, such as distillation and absorption processes, the best performance is usually obtained with packing techniques that involve a low pressure drop, good mass transfer efficiency, and high capacity. The objective for a new packing design, as discussed here, is to obtain a significant gas–liquid contact boundary (in other words, a large effective area) with low pressure drops for gas velocities in the range of 1–2 m s^{-1}. There has been significant evolution in the forms of structured packing over the last 30 years, the aim being to obtain the best trade-offs between capacity and efficiency. The basic geometry of structured packing was established by Meier (1981) for Sulzer Brothers Ltd. These packing materials were composed of corrugated metal (or wire-cloth) with perforations that improved the liquid distribution. The specific area of such packing varied from 125 to 700 $m^2\,m^{-3}$. The first improvement consisted of altering the packing surface with roughness or perforations intended to introduce turbulence. For example, McKeigue and Natarajan (1997) inserted openings by cutting two small strips. The second improvement was to machine elements with different shapes. Schultes (1999) and Pagade (2002) used this technique to make packing with new shapes and elements that had small thicknesses. Furthermore, Irwin et al. (2002) improved packing performance by placing a plane wall between corrugated metal sheets to increase the effective area. Finally, Hayashida et al. (2002) constructed packing with internal honeycomb structures composed of straight tubes in order to decrease the pressure drop.

Random packings have developed in a similar way. They are usually used in distillation or absorption processes. Their manufacturing techniques are even older and they have a lower effective area and a higher pressure drop. However, the liquid distribution is easier and they are cheaper overall. The first random packings had a simple shape, such as Raschig rings. The shapes are now more complex, such as Pall rings, CMRs (cascade mini rings), or IMPTs (Strigle and Porter, 1977), with thicknesses as small as in structured packing.

The new carbon structured packing suggested here extends the logical evolution of the packing structures described above. The important properties of an efficient packing seem to be a high effective area, good liquid distribution, good gas–liquid mixing, a low pressure drop, and a structure composed of a material of small thickness. In this paper, we present the different experimental steps necessary to characterize the new packing structure. In particular, the hydrodynamic performance in terms of pressure drop and flooding point, and the mass-transfer efficiency are determined.

2. Packing structure

This study focuses on a new structured packing technique (SPS Patent, 2005) developed by Snecma Propulsion Solide (the SAFRAN group). It is constructed of interwoven carbon fibres (Fig. 1). The tubes are formed with carbon fabrics, which are

* Corresponding author.
E-mail address: david.rouzineau@ensiacet.fr (D. Rouzineau).

woven on a mandrel according to a particular braid angle (Fig. 2a). The braid angle (θ) corresponds to the angle formed between a braid thread and the braid axis (Fig. 2b).

The distance between two fibre crossings (Fig. 2c) along the circumference is given by

$$AB = \frac{2\pi D_m}{N_f} \tag{1}$$

where D_m is the diameter of the mandrel (equivalent to the diameter of a tube) and N_f is the number of spindles (Fig. 2a, 16 spindles). If

$$AB \leq \frac{L_f}{\cos\theta} \tag{2}$$

where L_f is the width of a carbon fabric, there is no free space between the fibres (there is no hole), but if

$$AB > \frac{L_f}{\cos\theta} \tag{3}$$

a hole is formed. Fig. 3 represents a tube with holes. Thus, the value of the braid angle determines the tube hole sizes and the lower the braid angle, the bigger the holes. For example, for fibres with a width of 1 mm, a mandrel diameter of 15 mm, and 8 spindles, Fig. 4 shows the change in the surface area of the holes versus the braid angle.

The diameter of the mandrel can vary from 4.5 to 20 mm and the braid angle can vary from 15° to 45°. The openings therefore range from 0% to 85%, corresponding to a hole surface area from 0 to 735 mm^2. The percentage open surface of the tube is given by the squared meter of tube surface.

The tubes are then fitted together according to the four diagonals of a cube as shown in Fig. 5a, which demonstrates why this packing is called "Sepcarb® 4D packing". Finally, the layout is repeated in the three spatial directions (Fig. 5b) to obtain the final structure (Fig. 5c).

In the first step, the tubes are held together with epoxy resin. In the second step, the final structure is put in an oven to convert the resin into carbon and to achieve a carbon–carbon composite packing.

A first generation of packing structures with a diameter of 145 mm and a height of 50 mm was made with 10-mm-diameter tubes, a braid angle of 30°, and a hole size of 7.4 mm^2 (corresponding to an approximate opening of 30%; Fig. 6). This packing possessed a void fraction of approximately 94% and a specific surface area (a) of 420 m^2 m^{-3}. The surface area was evaluated by a geometrical calculation, knowing the surface area of the tubes, the diameter of the holes, and the number of tubes per cubic metre of packing.

This structure is advantageous because many parameters can be modified at will to optimize the performance of the structured

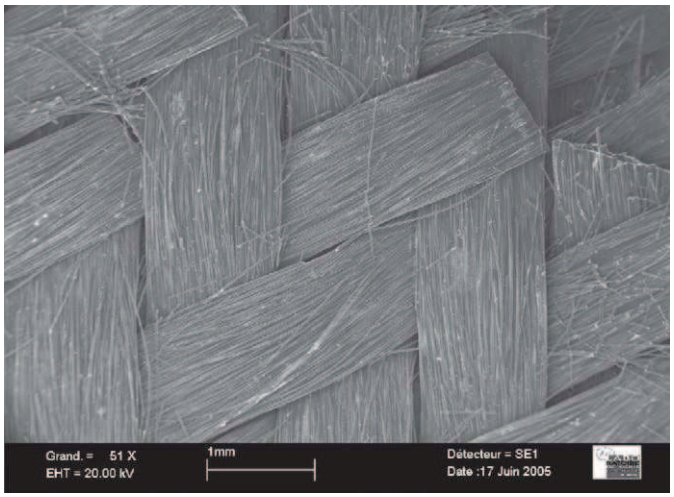

Fig. 1. Woven carbon fibres.

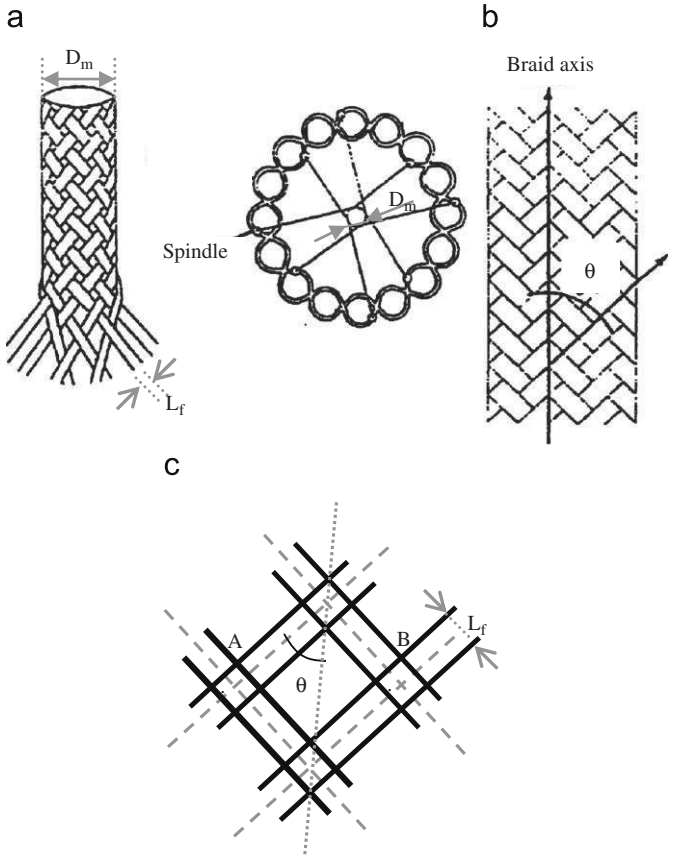

Fig. 2. (a) Carbon fabrics woven on a mandrel, (b) Braid angle, and (c) crossing of fibres.

Fig. 3. One tube with holes.

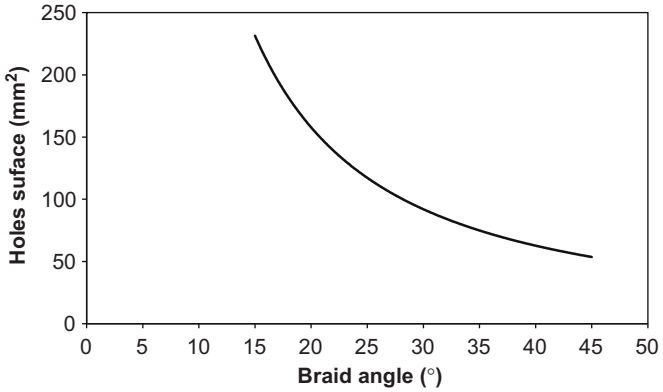

Fig. 4. Variation of hole surface area with braid angle.

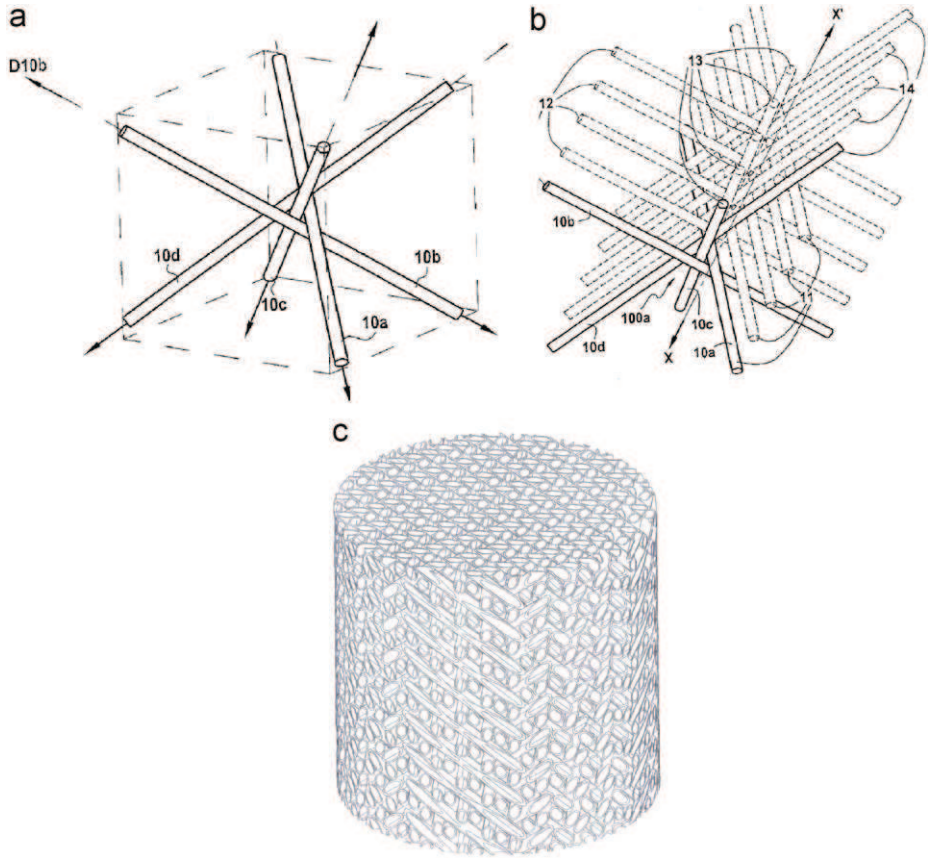

Fig. 5. (a) Tubes fitting according to the four diagonals of a cube, (b) reproduction of the layout in one direction, and (c) final structure.

Fig. 6. Sepcarb® 4D packing.

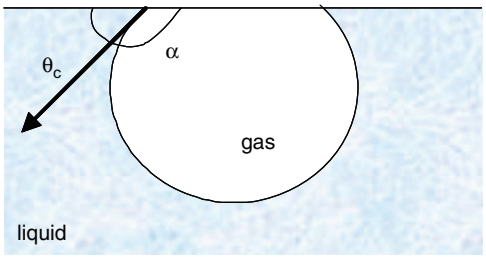

Fig. 7. Method of wettability measurement.

packing. In particular, it is possible to change the tube diameters, the hole sizes of tubes (openings), the sizes of carbon fabric (number of fibres), and the tube angles. Moreover, this packing possesses other interesting properties such as a small tube thickness (0.2 mm), as mentioned in the description of the evolution of structured packing, and significant structural cohesion (mechanical strength) due to the geometry of the structure (using of the four diagonals of a cube).

3. Material of the packing

Another important and interesting property of the Sepcarb® 4D packing is the material of the packing. Carbon is an inert, light, and corrosion-resistant material. Furthermore, the wettability of the carbon fibres yields promising results. This parameter is important to make sure that the liquid flows as a film in the separation unit, which ensures the efficiency of the packing.

For this material, the wettability was measured by forming a bubble under the material in order to measure the gas–solid angle (α); the liquid–solid angle (θ_c) being equal to $180-\alpha$ (Fig. 7). This method was best for this material because a drop would spread by capillary action between the fibres. The size of the bubble was in the 2–3 mm range. This method was used not only for a carbon specimen but also for stainless steel and Teflon (PTFE) in order to compare with two other common packing materials, which are well known to have good and bad water wettability, respectively.

Table 1 shows the wettability results; the values satisfy the efficient wettability criteria for film flow.

The measurement of a drop spreading on a solid surface is more efficient than the measurement of a bubble spreading on a flooded surface because it is a better representation of reality in this case. Moreover, the contact angles are relative to the static conditions whereas, in the operating conditions, it is the dynamic

contact angle that has to be considered. Therefore, these results must thus be regarded as indicative only.

These characteristics lead us to believe that this packing will be useful for gas–liquid contact in separation units.

4. Experimental setup and methods

4.1. Hydrodynamics

4.1.1. Pilot plant

The experimental hydrodynamics setup for this study is shown in Fig. 8. Eighteen 50-mm-high packing cylinders were placed in a glass column with an internal diameter of 150 mm in order to have a packing height of 900 mm. Counter current operation with an air–water system was used and all studies were carried out at room temperature and under standard atmospheric pressure. The packing was placed only in the upper part of a 2-m-high column; the other 1 m below the packing was used to reduce the influence of the perturbations caused by the liquid level in the bottom of the column.

The liquid flowed from a tank through a pump and flowmeter (with a measurement precision of $\pm 2.5\%$) and was fed into the top of the column via a liquid distributor with 283 holes per square metre. Two different liquid distributors (provided by Sulzer) were necessary to work properly in the range of *F*-factor from 0 to 3 $Pa^{0.5}$ (the first one for 0–1 $Pa^{0.5}$ range and the second one for 1–3 $Pa^{0.5}$ range). The liquid was collected back into the tank after having passed through the packing, with superficial liquid velocities in the range of 1–30 $m^3\,m^{-2}\,h^{-1}$. The gas flow was supplied at the bottom of the column and was measured by flowmeters (with a precision $\pm 1.6\%$) for superficial gas velocities from 0 to 2 $m\,s^{-1}$ for an empty column. The pressure drop per metre was measured using an inclined U-tube filled with water, which yielded pressure measurements with a precision of 0.05 mbar.

Table 1
θ_c angles of bubbles to characterize the Sepcarb® 4D packing wettability.

Material	4D	Stainless steel 304	Teflon
Water (deg)	6.25	35.4	94.4
Heptane (deg)	52.5	34.4	45.8

4.1.2. Method for hydrodynamics study

The experimental procedure used to measure the pressure drop consisted of a periodic increase of gas flow for a constant liquid flow until flooding was reached. The flooding point could be defined as the point where a reversal of liquid flow appeared. At this moment, the liquid was unable to flow downward through the packing, the pressure drop increased drastically, and an accurate pressure measurement was impossible due to the instability of the system. Before each test, a high liquid flow was supplied and passed through the bed for 30 min to fully wet the packing and avoid dry zones.

4.2. Mass transfer

4.2.1. Distillation pilot plant

The HETP experiments were performed with the distillation pilot plant described in Fig. 9 and Table 2. The mixture in the reboiler was heated with steam using a 60 kW electrical generator at 8 bar of maximum vapour pressure. The reboiler heat duty was calculated by measuring the condensate flow of water at its exit. The temperature at the reboiler and the head of the column was measured using thermocouples. Fractionation Research Inc. (FRI) and Separation Research Program (SPR) define standards for the experimental methods of separating a binary mixture by distillation at total reflux. This procedure consists of first reaching the flood point, then backing off to roughly 20% of the flood flowrate to unload the bed, and then running the test at the targeted reboiler duty. The different runs are carried out at atmospheric pressure with a standard cyclohexane/n-heptane mixture (Subawalla et al., 1997; Olujic et al., 2000). The range of reboiler duty is estimated by the corresponding hydrodynamics results. The tests were performed in the range of 2–8 kW and heat losses of the pilot plant were estimated beforehand at around 1.25 ± 0.11 kW.

The first tests were carried out with some well-known packings, 15×15 mm^2 Raschig glass rings, to validate the methods.

Liquid samples were taken from both the top and bottom of the column and analysed by refractometry. The time between the first vapour release and the first sample was almost 3 h, and steady state was considered to be achieved when three successive samples had identical compositions. Both top and bottom compositions were used to calculate the number

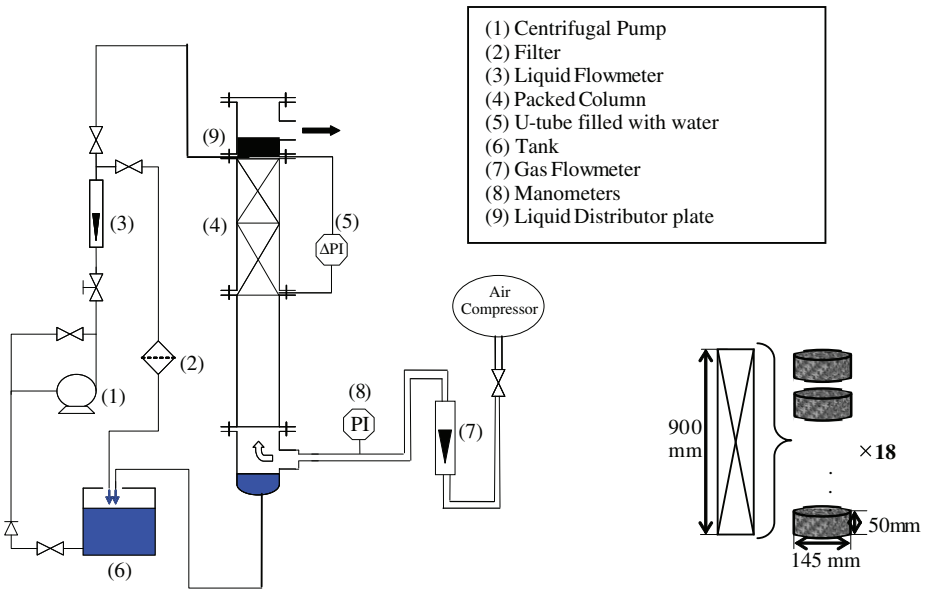

Fig. 8. Experimental setup for hydraulics experiments.

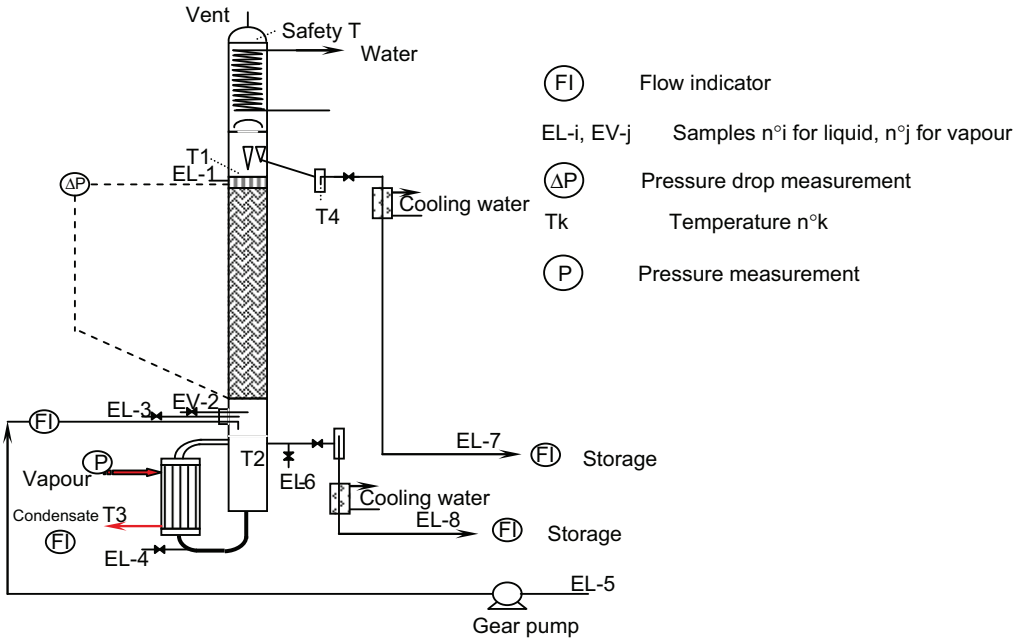

Fig. 9. Experimental setup for HEPT experiments.

Table 2
Experimental setup.

Reboiler	Volume: 13 l Vapour thermosiphon exchanger
Column	Diameter: 150 mm Packing height: 0.9 m
Head of column	Water condenser Sulzer liquid distributor plate (the same pf hydrodynamics tests)
Boiler	Vapour Maximum electric-power: 60 kW
Measures	Liquid samples Top of packing EL-1 Bottom of packing EL-3 Feed EL-5 Reboiler EL-4 EL-6 Distillate EL-7 Residue EL-8 Vapours samples Bottom of packing EV-2 Liquid temperatures Top of packing T1 Reboiler T2 Condensate T3 Distillate T4 Pressure Pressure drop over the packing Vapour inlet of exchanger Flow Distillate Residue Condensate outlet of exchanger
Feeds	At the bottom and the top of packing Gear pump
Outlets	Distillate: gravity flow Waste: gravity flow

of equilibrium stages (NTS). The mass transfer efficiency is reported in terms of the height equivalent of theoretical plate (HETP), the calculation of which is explained in detail in Section 4.2.2.

The pressure drop and HETP are presented as a function of the *F*-factor (vapour load) defined as the product of the superficial vapour velocity and square root of the vapour density, or

$$F = u_G \sqrt{(\rho_G)} \tag{4}$$

For the distillation results, the *F*-factor calculated at the top of the column was used.

4.2.2. HETP calculation

For each experiment, the HETP was determined by

$$\text{HETP} = \frac{\text{Packing height}}{\text{NTS}} \tag{5}$$

The value of the number of theoretical stages (NTS) can be calculated using the Fenske equation (based on the assumption of constant volatility), namely

$$\text{NTS} = \frac{\ln(x_d/1-x_d \times 1-x_w/x_w)}{\ln\alpha_m} \tag{6}$$

where α_m is the relative volatility of the mixture, and x_d and x_w are the compositions of the head and bottom of the column (the distillate and boiler). However, given the technology of the boiler (thermosiphon with circulation), it was not possible to obtain a sample with a composition corresponding to the fraction x_w from the Fenske equation. Therefore, the NTS was calculated as explained in Fig. 10. The proposed procedure avoids the constant volatility assumption. The experiments were carried out at total reflux, so the molar liquid fraction x_0 (EL-1) was equal to the vapour molar fraction y_1. With this value, the liquid molar fraction of the outlet of the first stage (x_1) was calculated using the equilibrium curve of the cyclohexane/n-heptane system. The vapour fraction y_2 was calculated by mass balance on stage 1. Because of the total reflux, the liquid flow was equal to the vapour flow, hence $y_2 = x_1$.

This methodology was followed at each stage until the liquid molar fraction x_n of stage number n became lower than the composition measured at the bottom of the column (EL-3). The theoretical stage number was then equal to $n-1$ plus the fraction of the stage needed to obtain a calculated value equal to the

measured composition. In other words,

$$\mathrm{NTS} = (n-1) + \left(\frac{x_{n-1} - x_w}{x_{n-1} - x_n}\right) \quad (7)$$

An example of a calculation (the fourth experiment) is presented in Appendix A.

5. Results and discussion

5.1. Hydrodynamics: pressure drop results

The experimental data obtained for dry packing are presented in Fig. 11 and the results for irrigated packing are presented in Fig. 12a and b. Eight experiments were performed to compare the pressure drop over wetted packing, with a variation of the liquid flow from 1 to 30 $m^3\,m^{-2}\,h^{-1}$ and a gas flow from 1700 to 11000 $m^3\,m^{-2}\,h^{-1}$, equivalent to an *F*-factor variation from 0.5 to 3.5 $Pa^{0.5}$.

First, it is noteworthy that the order of magnitude for the pressure drop per metre was in the range of a few millibars for the gas flows considered here. This result is quite acceptable for both distillation and absorption applications. Moreover, the trends are similar to classical trends observed for structured packing, where the pressure drop is proportional to the square of the gas flow (for a given liquid load). This can be observed from the straight line slope of 2 in Figs. 11 and 12a. A delineating break that separates the curve into two distinct zones appears with a higher increase of pressure drop, as shown in Fig. 12a. This point corresponds to the loading point. When the gas flow increases, the gas velocity disturbs the liquid gravity flow, the hold-up increases, and the available flow area for up-flowing vapour is reduced as the pressure drop increases. If the gas flow continues to increase, the hold-up increases until the flooding point is reached, corresponding to the last point of each curve (Fig. 12a and b). For the example shown in Fig. 12a, the slope change (equivalent to the loading point) occurs for an *F*-factor of 1.2 $Pa^{0.5}$, which corresponds to approximately 60% of the flooding point (where $F = 1.9\ Pa^{0.5}$).

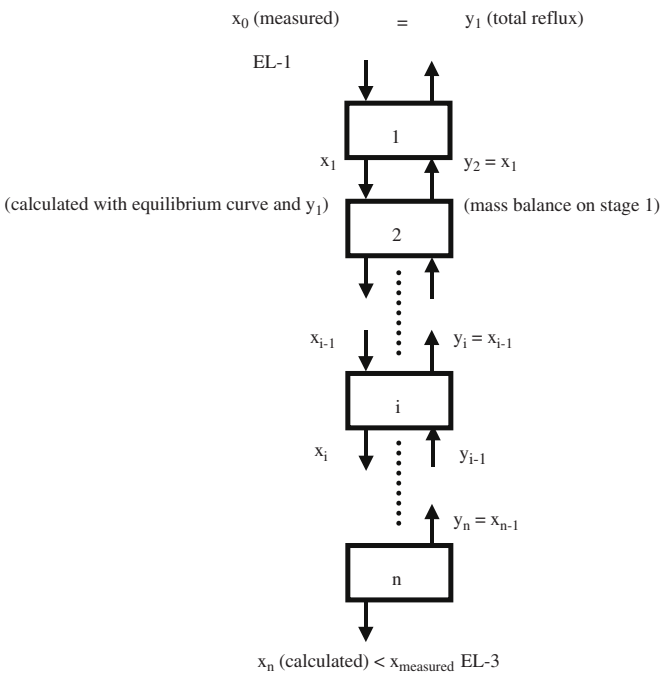

Fig. 10. Methodology of the NET calculation.

It is noticeable in Fig. 12b that the hydrodynamics behaviour is the same for each liquid flow. In fact, the curves are nearly parallel, the only significant difference coming from the increase in the pressure drop for an increase of liquid load, since the gas flow cross-section decreases.

The way in which the new structure Sepcarb® 4D generates a pressure drop is explained in Section 6.1.

5.2. Separation efficiency

The HETP was determined with gas flow variations from 170 to 3200 $m^3\,m^{-2}\,h^{-1}$ (equivalent to an *F*-factor from 0.08 to 1.6 $Pa^{0.5}$). The results are presented in Fig. 15 and in Table 3.

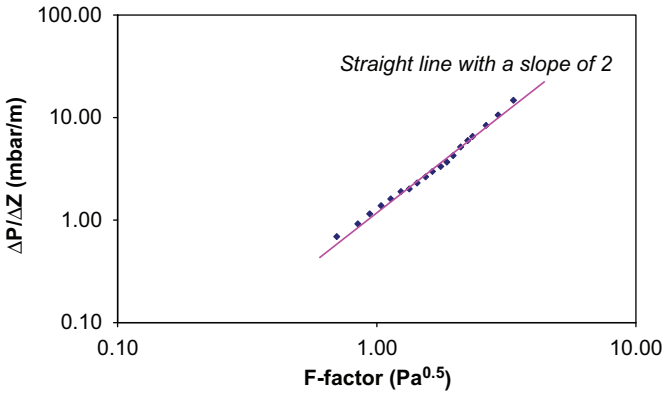

Fig. 11. Pressure drop over dry packing.

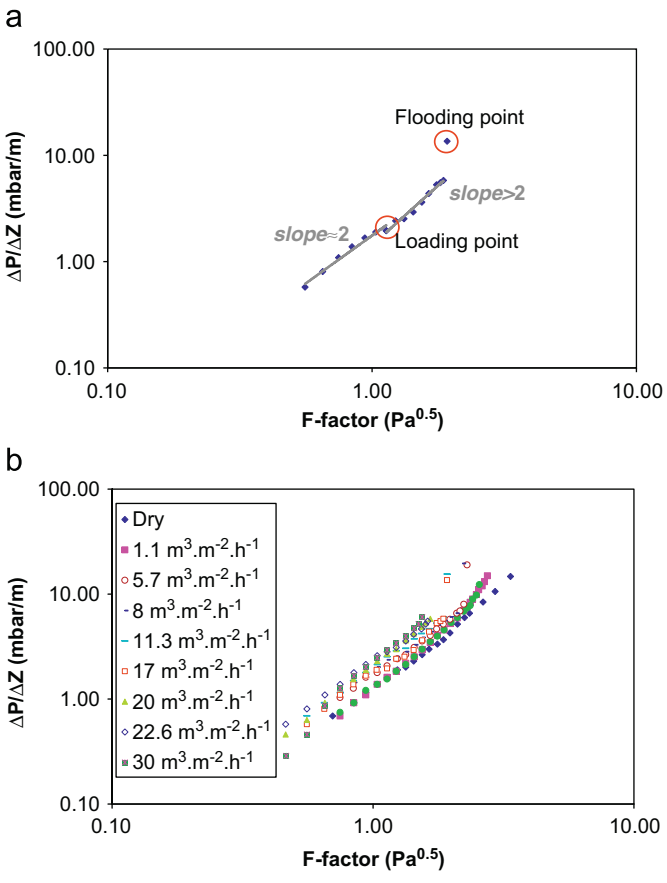

Fig. 12. (a) Pressure drop vs. gas *F*-factor for a liquid flow of 17 $m^3\,m^{-2}\,h^{-1}$ and (b) pressure drop vs. gas *F*-factor for different liquid flows.

First experiments were performed with carbon fabric around each packing segment as described in Fig. 13 to minimize the flow between the wall of the column and the packing.

The HETP was approximately 0.4 m, corresponding to 2.5 theoretical stages per metre, for a variation of the *F*-factor from 0.15 to 1.6 $Pa^{0.5}$ (corresponding to an equivalent gas flow from 320 to 3200 $m^3\,m^{-2}\,h^{-1}$). The curve (Fig. 15) shows a decrease in the HETP for an increase in the *F*-factor (i.e. when the flow through the column is greater). This result indicates a poor overall transfer efficiency. In fact, significant liquid flow was observed along the wall of the column because the carbon fabric was not waterproof. The liquid distribution on the packing was very poor, leading to poor separation efficiency.

In order to improve the liquid distribution and to further limit the flow between the wall of the column and the packing, wall wipers were placed between packing segments (Fig. 14).

For these trials, the average HETP was 0.2 m, yielding 5 theoretical stages per metre, for an *F*-factor variation from 0.1 to 1.3 $Pa^{0.5}$ (equivalent to a gas flow from 170 to 2600 $m^3\,m^{-2}\,h^{-1}$), which is a good result for structured packing. These results show that the performance was improved; in fact, the mass transfer efficiency was 100% higher with the wall wipers.

The experiments lead to the conclusion that redistribution and wall effects are important parameters to be considered for optimising the transfer efficiency in such a column with a diameter of 150 mm. However, it is possible to suppose that, with an industrial scale application (with a larger diameter), wall effects would have less influence and wall wipers would only prevent excessive wall flow rather than generate any considerable redistribution between packing segments.

6. Comparison with classical packings

In order to estimate the quality of the performance characteristics of Sepcarb® 4D packing, some comparisons were made with standard commercial packings. Three types of packing were chosen for the comparison: one random packing and two structured packings. These were, respectively,

- Sulzer Pall rings 5/8 in., denoted in diagrams by P-ring 5/8 (a=360 $m^2\,m^{-3}$); the dimensions are representative of packing materials commonly used in 150 mm diameter columns
- Sulzer Mellapak 250Y (a=250 $m^2\,m^{-3}$), widely used in industry
- Sulzer Mellapak 452Y (a=450 $m^2\,m^{-3}$), because the surface area is close to that of Sepcarb® 4D.

Table 3
Experimental results for separation efficiency.

	1st series	2nd series
Wall wiper	–	×
HETP (m)	0.4	0.2
NTS/m	2.5	5.0

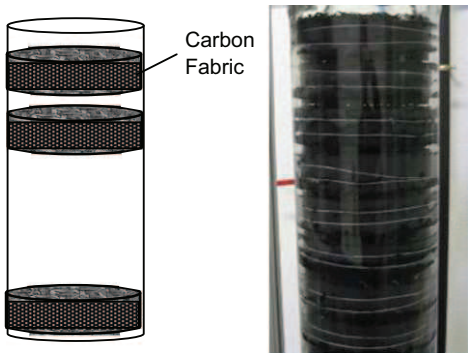

Fig. 13. Packing setup of 1st series of runs.

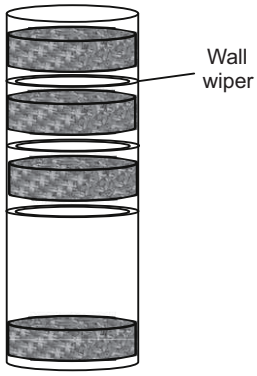

Fig. 14. Packing setup of 2nd series of runs.

6.1. Hydrodynamics comparison

Two points of comparison are usually used when comparing with standard packing: specific pressure drop vs. gas flow or gas *F*-factors for different liquid flows, and the liquid–gas loading factor from flooding results. The Sulzer Sulcol software [1.0, 2006] was used to obtain the hydrodynamic characteristics of each packing in order to have an idea of the performance level of this new structured packing.

Fig. 16 shows the pressure drop of the Sepcarb® 4D packing compared with the other packings for a liquid load of 7 $m^3\,m^{-2}\,s^{-1}$. The pressure drop is lower than that found for random packings using P-rings. However, it is higher than the pressure drop of the Sulzer Mellapak 250Y and of the Mellapak 452Y.

For the Mellapk 250Y, this can be explained by the higher specific area of the Sepcarb® 4D packing with respect to the Mellapak 250Y: 420 and 250 $m^2\,m^{-3}$, respectively. A greater surface area of materials obviously creates a greater pressure drop.

Regarding the Mellapak 452Y, the difference from the pressure drop with Sepcarb® 4D cannot be explained just by the small difference in surface area. The interesting question here is how this new Sepcarb® 4D structure generates the pressure drop. In Mellapak corrugated sheet structured packings, there are at least three governing sources: the contact points between the sheets, the direction changes due to the undulations of the structured corrugated sheets, and the fluid surface friction, which has the smallest influence. The structure of Sepcarb® 4D is different but the sources of pressure drop would remain the same, i.e. in increasing order of responsibility:

- Friction during direction change, due to the forced flow in inclined tubes. The inclination of the tubes (40° from the horizontal) is higher than the inclination of corrugations in a structured packing (more than 45°); which is probably why the pressure drop is greater in the Sepcarb® 4D.
- Contact points between tubes.
- Pressure loss caused by friction through the openings and fluid surface.

Moreover, the liquid can pass through the holes of the tubes, creating droplets and thus generating another source of pressure drop.

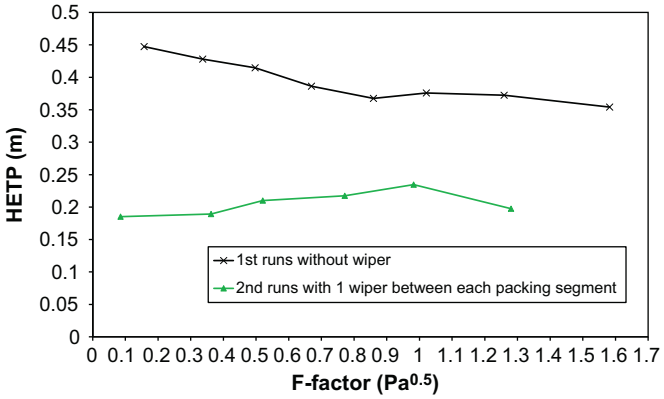

Fig. 15. Total reflux distillation performance results.

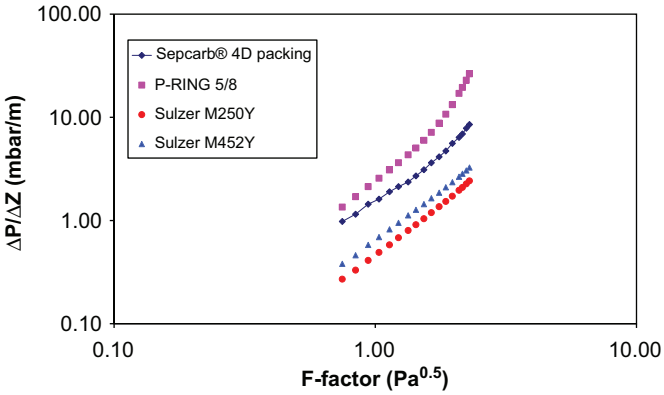

Fig. 16. Pressure drop comparison between different packings for a liquid flow of 7 $m^3\,m^{-2}\,h^{-1}$.

This analysis needs to complemented in further studies on the hydrodynamic behaviour by measuring the liquid phase distribution, because it has not been finalized here. These studies can be done either by numerical CFD calculations (Petre et al., 2003; Raynal and Royon-Lebeaud, 2007; Chen et al., 2009), by experimental measurements with intrusive methods based on fibre-optic sensors (Alekseenko et al., 2008), or non-intrusive methods using X-ray computed tomography (Toye et al., 1998; Aferka et al., 2007).

The flooding line is an important design parameter for a packing column because it determines the range of useful flows during distillation. To compare the performance of packings at flooding, the flowing factor at flooding, X (the x-coordinate of a Sherwood plot), and the capacity factor at flooding, Cg, were calculated as follows:

$$X = (L/\mathrm{Gf})\sqrt{(\rho_G/\rho_L)} \tag{8}$$

$$C_g = \frac{\mathrm{Gf}}{\sqrt{\rho_G(\rho_L-\rho_G)}} \tag{9}$$

Fig. 17 shows that, at the flooding point, the performance of Mellapak 250Y structured packing is superior to the performance of Sepcarb® 4D packing. Nevertheless, the Sepcarb® 4D packing has the same performance level as Mellapak 452Y. The gap between pressure drops can be explained by the holes in the tubes of the Sepcarb® 4D. These holes allow the liquid to pass through and thus the hydrodynamic behaviour (flooding) is different. Once again, it is difficult to conclude without a complete study of hydrodynamic behaviour using measurement of the liquid phase distribution.

The flooding point of the Sepcarb® 4D packing remains in the same range as for the other structured packings, so the application for a gas–liquid contactor is indeed possible.

The hydrodynamics tests demonstrate good performance of the first generation of Sepcarb® 4D packing in terms of the pressure drop (millibars per metre) and the flooding point. However, other generations of Sepcarb® 4D packing with different geometric parameters could be developed in order to optimize the pressure drop and flooding point, as dictated by a specific application.

6.2. HETP comparison

The separation efficiency results for the Sepcarb® 4D packing were then compared to the performance of the same three standard packings used in the hydrodynamics experiments (Fig. 18). The HETP used was from the second series. However, caution is necessary when interpreting the results since the column dimension, distillation system, and operating pressure were not the same for each packing; these results are just an indication to situate the separation efficiency of the new structured packing among commercial packings. The comparison products were the following:

- Sulzer M250Y with cyclohexane/n-heptane mixture at 1.65 bar (250 $m^2\,m^{-3}$ specific area) (Schultes and Chambers, 2007), in a 1.22 m diameter column with a packing height of 3.66 m.
- Pall ring 5/8 in. with methanol/2-propanol mixture at atmospheric pressure (360 $m^2\,m^{-3}$ specific area) (Wen et al., 2003), in a 0.15 m diameter column with a packing height of 1.23 m.

Moreover, to have a real point of comparison, experiments were performed with Sulzer Mellapak 452Y (450 $m^2\,m^{-3}$ specific area) in the same conditions and pilot plant as for the Sepcarb® 4D packing. Mellapak 452Y was used with collars around the packing, similar to those used in the industry. It is obvious from Fig. 18 that the Sepcarb® 4D packing has a lower HETP (and therefore a higher number of theoretical stages) than the Mellapak 250Y, the Mellapak 452Y and the Pall rings 5/8. This is in accordance with the specific area values. The comparison indicates that the Sepcarb® 4D packing has a good transfer efficiency with a lower HETP with respect to the classical packings. This result confirms that the capacity of the Sepcarb® 4D packing is sufficient for it to be used as a gas–liquid contactor in unit operations. Moreover, as explained previously, with experimental columns having a diameter greater than 150 mm, it is possible to improve the efficiency results because wall effects will be minimized and the HETP will probably be lower.

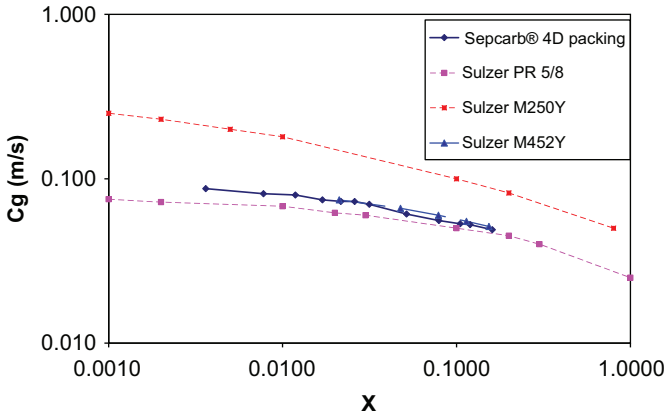

Fig. 17. Comparison of performance at flooding points.

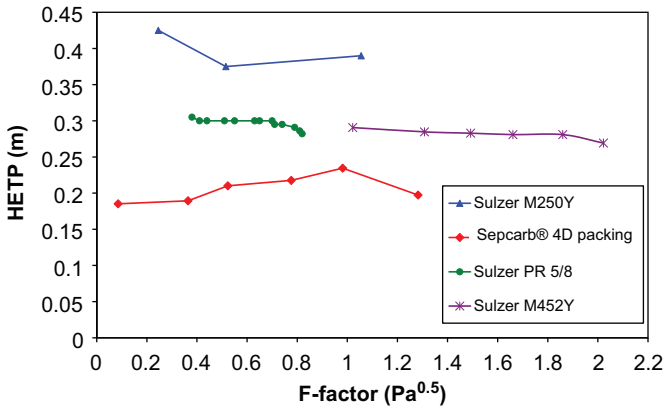

Fig. 18. Comparison of the HETP of the Sepcarb® 4D packing and standard packings.

7. New generation

The objective here was to see the influence of one geometrical parameter on the performance indicators in distillation, and particularly the pressure drop; therefore, a second generation of the Sepcarb® 4D packing was introduced. Several structure parameters had to be modified in order to reduce the pressure drop, such as the tube diameter or the opening. The chosen solution was to increase the size of holes (bigger openings). Therefore, the second generation of packing segments were made with the following characteristics: 145 mm diameter, 50 mm height, 10 mm tube diameter, braid angle of 30°. The second generation was similar to the first generation with only 8 spindles (N_f) instead of 12, so the hole size changed and became 26.6 mm^2 (relative to an approximate opening of 50%). This packing maintained a specific surface area (a) of 330 $m^2\ m^{-3}$.

Hydrodynamics and HETP experiments were performed to compare the performance of the two generations of Sepcarb® 4D packing.

7.1. Hydrodynamic tests

Experimental results were obtained for dry packing (presented in Fig. 19a) and for irrigated packing (presented in Fig. 19b). Four experiments were performed to compare the pressure drop over wet packing, varying the liquid flowrate from 11 to 30 $m^3\ m^{-2}\ h^{-1}$ and the gas flowrate from 1700 to 8000 $m^3\ m^{-2}\ h^{-1}$, equivalent to an F-factor variation of 0.65–2.5 $Pa^{0.5}$.

It is obvious from Fig. 19a and b that the trends are similar for both generations but, as expected, the pressure drop of the second generation, with an opening of 50%, is lower than the pressure drop of the first generation. For dry packing, an average gap of 40% is obtained, and for irrigated packing the results are improved by approximately 33%.

The increase in the size of holes allows the pressure drop to be decreased but it is important to know the impact on the transfer efficiency. Therefore, the HETP experiments with total reflux were run using the second generation of Sepcarb® 4D packing.

7.2. Separation efficiency

The tests were carried out without wall wipers in order to compare the results in the same conditions as for the Sulzer Mellapak 452Y. The HETP of the second generation packing was determined with a variation of the F-factor from 1 to 2.1 $Pa^{0.5}$. The pressure drop was measured and reported during the distillation experiments with the second generation of Sepcarb® 4D packing and the Mellapak 452Y. The results are presented in Fig. 20.

Fig. 20 shows that the transfer efficiency of the second generation (with 50% of opening) is better than that of the first generation (with 30% of opening) but is lower than that for M 452Y. Between the two generations of packing there is a gain of approximately 15% for an F-factor variation of 1–1.7 $Pa^{0.5}$. However, the results of the Sepcarb® 4D packing can be improved using a more appropriate contact between the packing and the wall of column as explained previously. It should be noted that the gap between the second generation of Sepcarb® 4D packing and Mellapak 452Y is low (less than 10%); the HETP per metre of both packings is around 0.3 (equivalent to NTS/m = 3.3), which corresponds to a good transfer efficiency in distillation.

Regarding the pressure drop, the values obtained with the two packings were in the same range, although the Mellapak 452Y provided a lower pressure drop than the second generation of Sepcarb® 4D. It is clear from Fig. 20 that the flooding point occurs for a lower F-factor in the second generation of packing than in the Sulzer packing. In fact, the flooding point seems to appear for an F-factor of approximately 2 $Pa^{0.5}$ using the Sepcarb® 4D packing.

These results show that the decrease in the specific area, due to the increase in the hole size, improves not only hydrodynamic performance but also transfer efficiency, probably thanks to hydrodynamic phenomena in the packing. With a decrease in specific area (from 420 to 330 $m^2\ m^{-3}$), the expected result would be a decrease in the transfer efficiency, but that is not what happened here. This could be explained by the fact that this

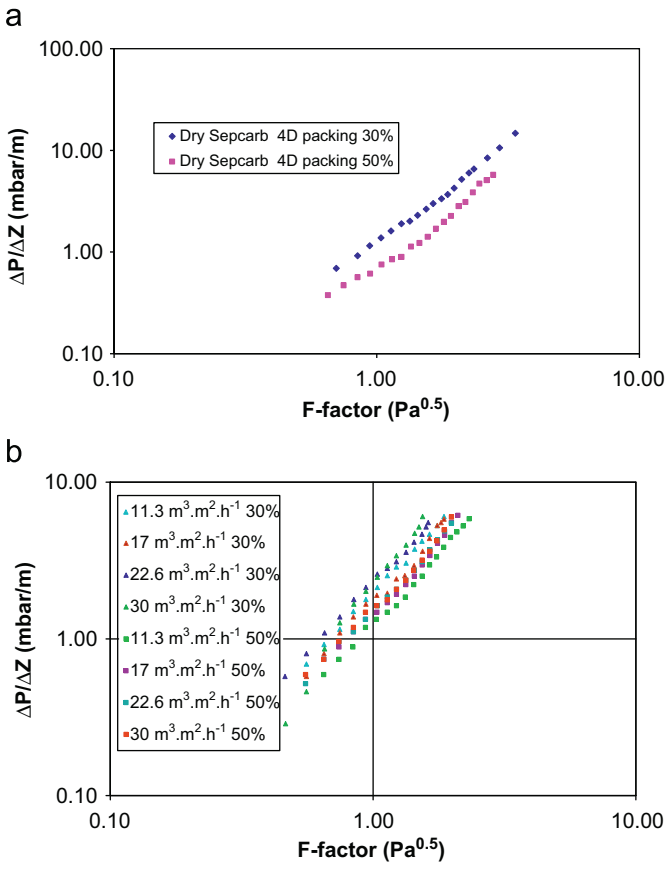

Fig. 19. (a) Pressure drop over dry packing for both generations and (b) pressure drop vs. gas F-factor for different liquid flows for both generations.

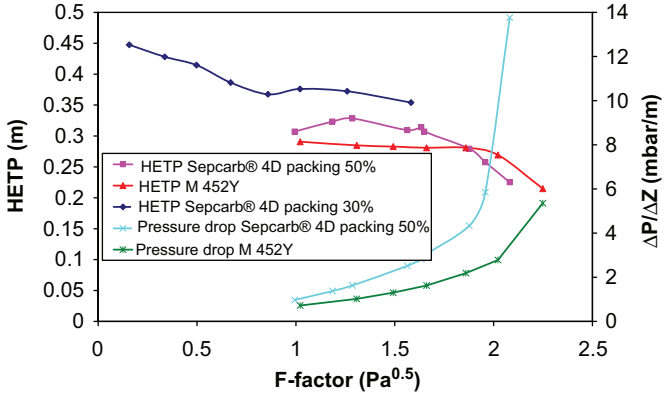

Fig. 20. Comparison of the HETP of the two generation of Sepcarb® 4D packing and Sulzer Mellapak 452Y.

packing does not behave in the same way as classical structured or random packings. As well as flowing in a film, the liquid passes through the holes, creating other gas–liquid contacts, like droplets, in addition to the contacts generated on the specific area of the packing. These generated droplets can participate in the mass transfer, and thus the interfacial area (a_e) can be higher than the specific area (a) for this packing, as has already been observed on IMTP (Intalox Metal Tower Packing) high capacity random packing (Alix and Raynal, 2009). Moreover, the large openings, 50% compared to the 30% between the two generations of packing, generate a higher, non-negligible amount of droplets. Hence, the interfacial area of 50% in the Sepcarb® 4D packing appears to be higher than the 30% one, leading to higher a_e/a ratios, and thus to lower HETP (Fig. 20).

The 50% Sepcarb® 4D packing structure could be more suitable than the 30% one since the efficiency is not affected by the opening while capacity is significantly increased. However, such a result should be validated later with effective area measurements. The air/NaOH system could be used to measure a_e (Seibert et al., 2005). For this system, it is assumed that the measured absorbed rate is directly linked to a_e.

8. Conclusion

Results for the efficiency of a new structured packing are presented in this paper. The main hydrodynamic characteristics of the packing, namely the pressure drop for dry and wetted packing and the flooding point, have been studied experimentally for a gas–liquid counter current flow with an air–water system. The measured pressure drop per unit height was in the range of a few millibars per metre, for an *F*-factor variation ranging from 0.5 to 3.5 $Pa^{0.5}$ (corresponding to an equivalent gas flow from 1700 to 11000 $m^3\,m^{-2}\,h^{-1}$), and for a liquid flow from 0 to 30 $m^3\,m^{-2}\,h^{-1}$. The pressure drop and flooding point show that hydrodynamic performance is somewhat lower when compared with the Mellapak 250Y and Mellapak 452Y and better than that with Pall rings. Therefore, it is possible to conclude that the results are in the range of the best commercial standard packings for classical *F*-factors (gas flow) and liquid flows.

The separation efficiency has been determined for the entire operating range using distillation experiments with a cyclohexane/n-heptane system at atmospheric pressure and total reflux. The HETP was calculated for two configurations aimed at optimising mass transfer performance. The best results were obtained with wall wipers, which improved the redistribution between packing cylinders and involved low wall effects. The HETP obtained was 0.2 m (equivalent to NTS per metre=5), which corresponds to a good transfer performance when compared to classical packings (M250Y, M452Y, and Pall rings).

vThe Sepcarb® 4D packing outlined here possesses very interesting internal properties due to its material and structure. Namely,

- Carbon is a corrosion-resistant, inert material.
- The packing has a very low density of approximately 40 kg per cubic metre.
- The packing has significant structural cohesion (mechanical strength).
- The tubes have a small thickness (0.2 mm).

Furthermore, the overall structure of the Sepcarb® 4D packing is very advantageous since it is possible to change various parameters to optimize performance. For example, the pressure drop needs to be low for CO_2 capture, which could be facilitated by having a bigger structure opening with larger size holes that would help to decrease the pressure drop involved. For a distillation application, the diameter of the tubes could be reduced in order to increase the specific area. Therefore, this packing can be easily adapted for a range of specific applications. To illustrate this property, a second generation of packing was made with a bigger opening to see the influence of the size of holes on the performance. With this packing, the hydrodynamic performance improved by about 35% and the mass transfer efficiency, the HETP, also improved by 15%.

Nomenclature

a	specific surface area (m^2/m^3)
AB	distance between two crossings of fibres
AC	compressed air
C_g	capacity factor (m/s)
D_m	diameter of the mandrel
EL-*i*, EV-*j*	no. of samples, *i* for liquid, *j* for vapour
F-factor	vapour load factor ($Pa^{0.5}$)
FI	flow indicator
Gf	gas flow at flooding point ($kg/s/m^2$)
H	total packed height (m)
HETP	height of an equivalent theoretical plate (m)
L	liquid flow ($kg/s/m^2$)
L_f	width of carbon fabric
NTS	number of theoretical stages
N_f	number of spindles
PI	pressure indicator
Tk	temperature n°k (K)
U_G	superficial gas velocity (m/s)
X	*x*-coordinate of Sherwood plot
x_d	composition of the distillate
x_w	composition of the waste

Greek letters

α	gas–solid angle
α_m	relative volatility of the mixture
ε	void fraction (%)
θ	braid angle (°)
θ_c	liquid–solid angle (°)
ΔP	pressure drop (mbar)
ΔPI	pressure drop indicator

ΔZ height difference (m)
ρ_G, ρ_L gas and liquid densities (kg/m^3)

Acknowledgements

The authors would like to thank Snecma Propulsion Solide and Sulzer for their help developing the new structured packing, and also for financial support and helpful discussions.

Appendix A. Example of a HETP calculation: fourth run with *F*-factor = 1.28 Pa$^{0.5}$

See appendix Table A1 here.

Table A1

Measurements		
T1, $T_{\text{top of the column}}$ (°C)	82.4	
T2, $T_{\text{bottom of the column}}$ (°C)	91.8	
Qb (kW)	14.4	
$X'_{W'}$ (EL-3)	0.36	
$X'_{d'}$ (EL-1)	0.85	
$X'_{\text{bouilleur}}$ (EL-4)	0.26	
$Y_{\text{bottom of the column}}$ (EV-2)	0.38	
HETP calculations		
No. of stage	*X*	*Y*
0	0.85	0.91
1	0.78	0.85
2	0.68	0.78
3	0.56	0.68
4	0.43	0.56
5	0.3	0.43
($X_5 < X_w$)		
ΔX ($X_4 - X_5$)	0.13	
$\Delta' X$ ($X_4 - X_w$)	0.07	
Fraction of theoretical stage ($\Delta' X/\Delta X$)	0.56	

NTS = 4.56 (=4+fraction of theoretical stage).
HETP = 0.197 m (=packing height/NTS).

References

Aferka, S., Crine, M., Saroha, A.K., Toye, D., Marchot, P., 2007. In situ measurements of the static liquid holdup in Katapak-SP12™ packed column using X-ray tomography. Chemical Engineering Science 62 (21), 6076–6080.

Alekseenko, S.V., Markovich, D.M., Evseev, A.R., Bobylev, A.V., Tarasov, B.V., Karsten, V.M., 2008. Experimental investigation of liquid distribution over structured packing. AIChE Journal 54 (6), 1424–1430.

Alix, P., Raynal, L., 2009. Pressure drop and mass transfer of a high capacity random packing. Application to CO_2 post-combustion capture. Energy Procedia 1 (1), 845–852.

Chen, J., Liu, C., Yuan, X., Yu, G., 2009. CFD simulation of flow and mass transfer in structured packing distillation columns. Chinese Journal of Chemical Engineering 17 (3), 381–388.

Hayashida, S., Kihara, H., Kawakami H., 2002. Vapor–liquid contactor, cryogenic air separation unit and method of gas separation, Nippon Sanso Corporation, US 2002/0157537.

Irwin, N.C., Krishnamurphy, R., McKeigue, K., 2002. Structured packing. US 2002/014130.

McKeigue, K., Natarajan, V., 1997. Structured Packing. The BOC Group Inc., US 5.624.733.

Meier, W., 1981. Packing Element for an Exchange Column. Sulzer Brothers Ltd., US 4.296.050.

Olujic, Z., Seibert, A.F., Fair, J.R., 2000. Influence of corrugation geometry on the performance of structured packings: an experimental study. Chemical Engineering and Processing 39, 335–342.

Pagade, K.P., 2002. Fluid contacting device used as structured packing and static mixer. US2202/0063344.

Petre, C.F., Larachi, F., Iliuta, I., Grandjean, B.P.A., 2003. Pressure drop through structured packings: breakdown into the contributing mechanisms by CFD modeling. Chemical Engineering Science 58 (1), 163–177.

Raynal, L., Royon-Lebeaud, A., 2007. A multi-scale approach for CFD calculations of gas–liquid flow within large size column equipped with structured packing. Chemical Engineering Science 62 (24), 7196–7204.

Seibert, F., Wilson, I., Lewis, C., Rochelle, G., 2005. The Greenhouse Gas Control Technologies II, 1925–1928.

Schultes, M., 1999. Packing Element for Use, in Particular, in Mass Transfer and/or Heat Transfer Columns or Towers. Raschig AG, US 5.882.772.

Schultes, M., Chambers, S., 2007. How to surpass conventional and high capacity structured packings with raschig super pak. Chemical Engineering Research and Design 85 (A1), 118–129.

SPS Patent: patent FR 0511051, 28/10/2005.

Strigle, R.F., Porter Jr., K.E., 1977. Tower Packing. Norton Company, US 4.303.599.

Subawalla, H., Castor Gonzalez, J., Seibert, A.F., Fair, J.R., 1997. Capacity and efficiency of reactive distillation bale packing: modeling and experimental validation. Industrial Engineering and Chemical Research 36, 3821–3832.

Toye, D., Marchot, P., Crine, M., Pelsser, M., L'Homme, G., 1998. Local measurements of void fraction and liquid holdup in packed columns using X-ray computed tomography. Chemical and Engineering Processing 37 (6), 511–520.

Wen, X., Afacan, A., Nandakumar, K., Chuang, K.T., 2003. Geometry-based model for predicting mass transfer in packed columns. Industrial Engineering and Chemical Research 42, 5373–5382.